HHS Public Access

Author manuscript

*Clin Nucl Med*. Author manuscript; available in PMC 2020 June 01.

Published in final edited form as:

*Clin Nucl Med*. 2019 June ; 44(6): 439–445. doi:10.1097/RLU.0000000000002584.

# $^{68}$Ga-NOTA-Evans Blue TOF PET/MR lymphoscintigraphy evaluation of the severity of lower limb lymphedema

**Guozhu Hou, MD**[#*,†], **Bo Hou, MD**[#‡], **Yuanyuan Jiang, MD**[#*,†], **Zhaohui Zhu, MD**[*,†], **Xiao Long, MD**[§], **Xiaoyuan Chen, PhD**[ξ], and **Wuying Cheng, MD**[*,†]

[*]Department of Nuclear Medicine, Peking Union Medical College (PUMC) Hospital, Academy of Medical Sciences and PUMC

[†]Beijing Key Laboratory of Molecular Targeted Diagnosis and Therapy in Nuclear Medicine

[‡]Department of Radiology, PUMC Hospital Chinese Academy of Medical Sciences and PUMC

[§]Department of Plastic Surgery, PUMC Hospital Chinese Academy of Medical Sciences and PUMC, Beijing, People's Republic of China

[ξ]Laboratory of Molecular Imaging and Nanomedicine, National Institute of Biomedical Imaging and Bioengineering, National Institutes of Health, Bethesda, MD.

[#] These authors contributed equally to this work.

## Abstract

**Purpose:** This study was designed to investigate the role of $^{68}$Ga-NOTA-Evans Blue (NEB) time-of-flight (TOF) positron emission tomography/magnetic resonance (PET/MR) in evaluating lower limb lymphedema by visual analysis and novel parameters.

**Methods:** Thirteen patients with unilateral lower limb lymphedema were divided into 3 groups according to the clinical severity: minimal (4 patients), moderate (5 patients), and severe (4 patients). All patients underwent $^{68}$Ga-NEB TOF PET/MR lymphoscintigraphy. The ratio of superficial lymphatic vessel (SLV)'s Standardized uptake value (SUV) vs deep lymphatic vessel (DVL)'s SUV ($SUV_{slv/dlv}$) was designed to assess the level of lymphedema severity. The correlation between lymphedema severity and lymphoscintigraphy findings was determined using one-way analysis of variance, the *t* test, and Pearson correlation analysis.

**Results:** There was a significant difference in the $SUV_{slv}$ between the affected limbs and normal limbs in all subjects (affected limbs: 0.57±0.32, normal limbs: 1.86±1.43, $P<0.05$), which was not found in the $SUV_{dlv}$ (affected limbs: 0.64±0.39, normal limbs: 0.63±0.31, $P>0.1$). The $SUV_{slv/dlv}$ of the affected limbs showed statistical differences within the three groups ($P<0.05$) (minimal group: 1.91±0.45; moderate group: 0.84±0.16; severe group: 0.42±0.11). The statistical analysis revealed a negative correlation between $SUV_{slv/dlv}$ and the severity of lymphedema ($r = -0.899$, $P<0.01$).

**Correspondence to:** Wuying Cheng, MD, Department of Nuclear Medicine, Peking Union Medical College Hospital, No. 1 Shuaifuyuan, Wangfujing St, Dongcheng District, Beijing 100730, People's Republic of China. cwypumch@126.com; Xiao Long, MD, Department of Plastic surgery, Peking Union Medical College Hospital, No. 1 Shuaifuyuan, Wangfujing St, Dongcheng District, Beijing 100730, People's Republic of China. pumchlongxiao@126.com; Xiaoyuan Chen, PhD, National Institutes of Health, 35A Convent Dr, GD937, Bethesda, MD 20892. shawn.chen@nih.gov.

**Conclusions:** $^{68}$Ga-NEB TOF PET/MR lymphoscintigraphy can provide anatomical and functional information of lymphatic vessels to guide surgery plans. $SUV_{slv/dlv}$ was well correlated with clinical lymphedema severity and might be potential in evaluating bilateral lower limb lymphedema.

### Keywords

$^{68}$Ga-NEB; PET/MR; Lymphedema; Lower limb

## Introduction

Lymphedema is a progressive, chronic condition.[1] Secondary lower limb lymphedema is mainly caused by lymph node dissection after pelvic malignant tumor resection.[2] Severe lower limb lymphedema significantly reduces the patient's quality of life, and even affect their mental health.[3, 4] Early detection and severity assessment of lymphedema, commonly based on changes in the circumferences or volume of affected limb compared to that of contralateral unaffected limb, facilitates early interventions (conservative or operative) and offers greater treatment success.[3, 5, 6] $^{99m}$Tc-sulfur colloid (SC) lymphoscintigraphy is the first-line imaging method to diagnose lymphedema.[7] Limb volume is correlated with the severity of lymphedema based on the International Society of Lymphology classification.[8] To forecast lymphedema severity, some methods measuring the limb volume has been used in clinics.[9, 10] Tape measurement is the most frequently used method for calculating limb volume clinically.[9, 10] Computed tomography (CT) and magnetic resonance (MR) imaging are helpful for measuring the subcutaneous volume of limbs, and both tools provide objective measurements in consideration of the effect of muscle disuse atrophy.[11, 12] Traditional measurement approaches play a certain role in evaluating the severity of unilateral lower limb lymphedema, while those measurements of limb volume have a common disadvantage that the patients with lymphedema must have a normal limb to be compared with the swollen limb. Clinical severity evaluation in cases of bilateral lower limb lymphedema presents a challenge to clinicians.[8]

$^{68}$Ga-NOTA-Evans Blue (NEB) time-of-flight (TOF) positron emission tomography (PET) lymphoscintigraphy has been used to evaluate lymphatic drainage function and provide guidance for microsurgery treatment schemes.[2] It is expected that $^{68}$Ga-NEB TOF PET/MR might present more detailed information about the anatomy and function of the lymphatic system.[13]

The purpose of this study was to investigate the role of $^{68}$Ga-NEB TOF PET/MR lymphoscintigraphy in guiding microsurgery schemes and the potential value of a new parameter, the ratio of superficial lymphatic vessel (SLV)'s Standardized uptake value (SUV) vs deep lymphatic vessel (DVL)'s SUV ($SUV_{slv/dlv}$), in evaluating the severity of bilateral lower limb lymphedema.

## Materials and methods

### Patient recruitment

This study was registered at clinicaltrials.gov (NCT03347864). All patients were recommended from the Department of Plastic Surgery, Peking Union Medical College Hospital (PUMCH). This clinical study was approved by the Institute Review Board of PUMCH and was conducted following the Declaration of Helsinki. All subjects signed written informed consent and were informed of the potential benefits and risks of participating in the investigation.

The inclusion criteria were patients (1) diagnosed with lymphedema of the unilateral lower limb based on $^{99m}$Tc-SC lymphoscintigraphy exhibiting an absence or reduction of radiolabeled colloid to the regional lymph nodes and/or dermal backflow and (2) aged no younger than 18 years old. The exclusion criteria were patients (1) with mental illness; (2) with severe liver or kidney dysfunction; (3) who were allergic to intravenous (IV) radiographic contrast; (4) with hematopoietic dysfunction; (5) with claustrophobia who could not undergo PET/MR scanning; and (6) who were female and pregnant or breast-feeding.

### Clinical severity

The volume variation was a common measurement for the severity of lymphedema as follows: minimal, the affected limb was 5%–20% larger in volume than the normal limb; moderate, the damaged limb was >20% larger in volume than the normal limb; and severe, the impaired limb was >40% larger in volume than the normal limb.[8, 14]

### Patients

Thirteen female patients with unilateral lower limb lymphedema were divided into 3 groups according to the clinical severity: minimal (4 patients), moderate (5 patients), and severe (4 patients). The average age of the patients was 48.6 ± 9.5 years. All patients underwent $^{99m}$Tc-SC scintigraphy for comparison within 2 weeks of undergoing $^{68}$Ga-NEB TOF PET/MR lymphoscintigraphy.

### Imaging protocols

$^{68}$Ga-NEB TOF PET/MR lymphoscintigraphy

All patients underwent TOF PET/MR 20 and 40 min after subcutaneous injections into the first interdigital spaces of both feet (0.5 mL, 37 MBq/foot).

All imaging acquisitions were performed using an integrated PET/MR scanner (SIGNA PET/MR, GE, Milwaukee, Wisconsin). With regard to the coverage from the ankle to the pelvic cavity and the limited PET acquisition coverage of 25 cm, the scanning was completed by 3 or 4 bed stations, depending on the exact coverage. The ordered-subsets expectation maximization algorithm was used for PET image reconstruction, and the parameters were the following: 12 iterations, 28 subsets, and full width at half maximum of a Gaussian filter of 6.0 mm. The PET images were reconstructed to a matrix of 192×192,

and the slice thickness was 2.94 mm. For each bed station, the MR protocol included axial T2-weighted imaging (T2WI) and T1-weighted imaging (T1WI) as follows: (1) T2WI with a fast recovery fast spin echo (FSE) sequence (repetition time (TR) = 5200 ms, echo time (TE) = 110 ms, field of view (FOV) = 50 cm × 40 cm, slice thickness = 6 mm, no slice spacing, matrix = 480 × 288), and the iterative decomposition of water and fat with echo asymmetry and least-squares estimation (IDEAL) method was used to achieve better fat saturation; and (2) T1WI with a FSE sequence (TR = 420 ms, TE = 10.3 ms, FOV = 50 cm × 40 cm, slice thickness = 5 mm, no slice spacing, matrix = 512 × 288), and IDEAL was also used to obtain separated water, fat, in-phase, and out-of-phase images. The scanning lasted about 6 min per the PET acquisition for each station. After imaging of all the stations, the scanning repeated from the first one. After the second acquisitions of all stations, coronal MR imaging with a large FOV was performed as follows: (1) fat-saturated single-shot FSE to achieve T2WI (TR = 2000 ms, TE = 50 ms, FOV = 50 cm × 50 cm, slice thickness = 5 mm, slice spacing = 1 mm, matrix = 352 × 224) and (2) T1WI with liver acquisition with volume acceleration-flex, TR = 4.2 ms, TE = 1.1 ms, FOV = 50 cm × 50 cm, slice thickness = 1.5 mm, matrix = 480 × 352) to achieve high resolution and homogeneous fat saturation.

### Imaging analysis and statistics

Visual and semi-quantitative methods were applied for image analysis. The images were analyzed and diagnosed by two experienced nuclear medicine physicians and two experienced radiologists together.

The visual method was used to evaluate the lymphatic system, including the number, location, and distribution of lymphatic vessels and glands.

(Regions of interest) ROIs were used to measure $SUV_{slv}$ and $SUV_{dlv}$. The middle of the crus, middle of the leg, and middle of the thigh were chosen as three key ROIs. The maximum SUV ($SUV_{max}$) of both SLVs and DLVs in the three regions were measured respectively. The $SUV_{slv}$ was set as the average $SUV_{slvmax}$ of these three regions. The $SUV_{dlv}$ was set as the average $SUV_{dlvmax}$ of these three regions Meanwhile, the ratio of $SUV_{slv}$ to $SUV_{dlv}$ ($SUV_{slv/dlv}$), a new parameter, was designed to assess the severity of lymphedema (Table 1). The SUV was calculated based on the dose of $^{68}$Ga-NEB and weight of the patients.

The correlation between lymphedema severity and $^{68}$Ga-NEB TOF PET/MR lymphoscintigraphy findings was determined using one-way analysis of variance, the *t* test, and Pearson correlation analysis. The results were expressed as $x \pm s$. SPSS 24.0 Software (IBM SPSS, Chicago, IL, USA) was used for statistical analyses.

## Results

The level of swelling in lower limbs with lymphedema increased from the minimal group to the severe group (Fig. 1a-1c). The qualitative image findings of $^{99m}$Tc-SC lymphoscintigraphy, like dermal backflow and decreased lymph node accumulation in the affected lower limbs, could be observed in all three groups (Fig. 1d-1f). Quantitative

lymphoscintigraphy analysis is not routinely applied in clinical practice due to its time-consuming and relatively complicated operating process.

The image findings of dermal backflow and decreased lymph node accumulation of affected limbs on $^{68}$Ga-NEB TOF PET/MR lymphoscintigraphy were similar to those on $^{99m}$Tc-SC lymphoscintigraphy (Fig. 2a-2f, Table 2). Moreover, the more important finding on $^{68}$Ga-NEB TOF PET/MR lymphoscintigraphy was the detailed visualization of SLVs and DLVs. SLVs of defected limbs demonstrated decreased tracer uptake than normal limbs on $^{68}$Ga-NEB TOF PET/MR, but DLVs in the normal and affected limbs showed the same degree of uptake in all subjects (Fig. 2a-2f). There was a significant difference in the $SUV_{slv}$ between the affected limbs and normal limbs (affected limbs: 0.57±0.32, normal limbs: 1.86±1.43, $P<0.05$, Fig. 3), but such a difference was not found in $SUV_{dlv}$ (affected limbs: 0.64±0.39, normal limbs: 0.63±0.31, $P>0.1$, Fig. 4). There were also much more adipose fat and tissue fibrosis deposition around the SLV than around the DLV.

$SUV_{slv/dlv}$ of affected limbs showed statistical differences among the three groups ($P<0.05$, Fig. 5) (minimal group: 1.91±0.45; moderate group: 0.84±0.16; severe group: 0.42±0.11). The statistical analysis revealed a negative correlation between $SUV_{slv/dlv}$ and the severity of lymphedema ($r = -0.899$, $P<0.01$).

## Discussion

The technique of injection is important for lymphoscintigraphy. $^{68}$Ga-NEB was subcutaneously injected into the first interdigital spaces of both feet where a wheal formed on the skin; after that, no blood was observed in the injector while withdrawing the plunger of the syringe, ensuring that $^{68}$Ga-NEB was injected into the subcutaneous tissue and absorbed by the lymphatic circulatory system.[15] When $^{68}$Ga-NEB is injected into subcutaneous tissue, it combines with endogenous proteins in the cellular matrix to form a $^{68}$Ga-NEB-protein complex, which can move to the lymphatic circulatory system through the monolayer endothelial cells of the lymphatic capillaries.[16, 17] However, the complex's size is too large to have access to blood circulation through vascular endothelial cells.[17, 18] Lymphedema is the result of an overload of lymph fluid that accumulates in the subcutaneous space, causing an increase in limb weight, decreased limb function, increased risk of infection, compromised quality of life, and interference with body appearance.[5, 19–22] Surgical interventions for limb lymphedema include lymphaticovenous anastomosis and vascularized lymph node transfer, which help reduce the excess fluid component of lymphedema.[23–25] Both surgery methods require correct severity assessment and maps of the lymph system.[26, 27]

The earlier that the detection and correct severity assessment of lymphedema are made, the greater the chances of identification of appropriate and functional vessels to manipulate, which is crucial for the success of surgery. The major advantage of $^{68}$Ga-NEB PET/MR lies in the effective combination of the ability of $^{68}$Ga-NEB PET and MR. $^{68}$Ga-NEB PET could quantify the function of the lymphatic system in the form of SUV, which is reflected in the $^{68}$Ga-NEB activity concentrations, and MR could point out the position and depth of lymphatic vessels with anatomic accuracy. $^{68}$Ga-NEB PET/MR imaging can provide the

precise location and $^{68}$Ga-NEB uptake levels in lymphatic vessels that are available to manipulate to guide microsurgery schemes.[2, 8, 18, 28–30]

Several studies have investigated the utility of $^{99m}$T-SC lymphoscintigraphy in the evaluation of lymphatic function through quantitative analysis and considered quantitative lymphoscintigraphy sensitive in detecting and grading lymphedema, while the correlation between lymphedema clinical severity and lymphoscintigraphic findings have yet to be discussed.[31–34] Besides that, the time-consuming and complex characteristic of quantitative lymphoscintigraphy has restricted its application in clinics. All thirteen patients in our study underwent $^{99m}$Tc-SC lymphoscintigraphy for comparison, and the images were interpreted using a qualitative analysis method. Qualitative imaging findings, like dermal backflow and reduced accumulation of visualized lymph nodes, could be observed in all three groups, making $^{99m}$Tc-SC lymphoscintigraphy not well correlated with clinical lymphedema severity. The study of Maclellan et al. including 134 patients with limb lymphedema investigated the relationship between clinical lymphedema severity and $^{99m}$Tc-SC lymphoscintigraphy findings (dermal backflow and transit time) and did not find any correlation, drawing a conclusion that a lymphoscintigram should be interpreted as normal or abnormal instead of reflecting clinical severity or function level.[35]

The severity assessment of unilateral lymphedema utilized simple volume differences between the affected limb and normal limb, while the assessment of bilateral limb lymphedema remains a particular challenge to clinicians. Conventional severity assessment approaches (tape measurement, MR or CT) of measuring affected limb volume excess compared to the normal limb are not possible in cases of bilateral lymphedema, wherein there is no unaffected contralateral limb to act as a reference.[4, 14, 26, 32, 36–40] The $SUV_{slv/dlv}$ of the affected limb showed statistical differences in the three groups ($P<0.05$), suggesting that the $SUV_{slv/dlv}$, which was based on deep and superficial lymphatic function, was related to clinical lymphedema severity. Therefore, $SUV_{slv/dlv}$ could be used to assess clinical lymphedema severity without knowing the circumference or volume of bilateral lower limbs, which are indispensable parameters for conventional methods. Based on this finding, $SUV_{slv/dlv}$ shows great promise for the evaluation of bilateral lymphedema.

There was no significant difference in the $SUV_{dlv}$ between the affected limb and normal limb ($P>0.1$), indicating that the deep lymphatic function of the affected limb, of which the superficial lymphatic function was impaired, was nearly as normal as that of the unaffected limb. We also observed that the adipose fat and tissue fibrosis commonly observed around the SLV barely appeared around the DLV. One probable reason for these findings might be the contractile function of the muscle wrapping around the DLVs. With the cause attributed to the contraction of muscles wrapping the DLVs, the drainage function of the DLVs would not be compromised greatly. The less chance of drainage functions of DLVs being impaired than that of SLVs might also explain why there are less fibrotic tissue and adipose fat depositions around the DLV than the SLV.

Some limitations of $^{68}$Ga-NEB TOF PET/MR lymphoscintigraphy must be illuminated. The number of subjects was not enough, and a large-scale clinical trial is expected. The patients included in this study were all female, and majority of those patients underwent pelvic

surgery. We provided descriptive results about the extent of subcutaneous adipose fat and tissue fibrosis, which was inconvenient to quantify. The $SUV_{slv/dlv}$ was inferred to have potential value in evaluating bilateral lymphedema, while patients recruited in this study all had unilateral lymphedema. Clinical trials including patients with bilateral lymphedema to further clarify the specific roles of the $SUV_{slv/dlv}$ are also expected.

## Conclusion

The severity of lymphedema might be evaluated by $^{68}$Ga-NEB TOF PET/MR lymphoscintigraphy, which was in accordance with the severity of lymphedema in patients with unilateral lymphedema in this study, so we expect that the $SUV_{slv/dlv}$ might be useful to assess the severity of lymphedema in patients with bilateral lower limb lymphedema. Moreover, $^{68}$Ga-NEB TOF PET/MR lymphoscintigraphy might provide information regarding the lymphatic system to guide lymphedema microsurgery schemes and postoperative follow-up. There was also an incidental discovery that the function of SLVs seems to be more likely affected than that of DLVs in lymphedema.

## Acknowledgments

**Conflicts of interest and sources of funding:** This work was supported by the National Nature Science Foundation of China (No.81371588; No.81670444); the Intramural Research Program (IRP) of the National Institute of Biomedical Imaging and Bioengineering (NIBIB), National Institutes of Health (NIH); Beijing Key Laboratory of Molecular Targeted Diagnosis and Therapy in Nuclear Medicine. The authors declare that they have no conflict of interest.

## References

1. Shimony A, Tidhar D. Lymphedema: a comprehensive review. Ann Plast Surg 2008;60:228.
2. Long X, Zhang J, Zhang D, et al. Microsurgery guided by sequential preoperative lymphography using (68)Ga-NEB PET and MRI in patients with lower-limb lymphedema. Eur J Nucl Med Mol Imaging. 2017;44:1501–1510. [PubMed: 28382512]
3. Lawenda BD, Mondry TE, Johnstone PA. Lymphedema: a primer on the identification and management of a chronic condition in oncologic treatment. CA Cancer J Clin 2009;59:8–24. [PubMed: 19147865]
4. Han DY, Cheng MF, Yen RF, et al. Postoperative lymphocele demonstrated by lymphoscintigraphy SPECT/CT. Clin Nucl Med 2012;37:374–376. [PubMed: 22391709]
5. Rockson SG, Rivera KK. Estimating the population burden of lymphedema. Ann N Y Acad Sci 2008;1131:147–154. [PubMed: 18519968]
6. Purushotham AD, Bennett Britton TM, Klevesath MB, et al. Lymph node status and breast cancer-related lymphedema. Ann Surg 2007;246:42–45. [PubMed: 17592289]
7. Neligan PC, Kung TA, Maki JH. MR lymphangiography in the treatment of lymphedema. J Surg Oncol 2017;115:18–22. [PubMed: 27377990]
8. The Diagnosis and Treatment of Peripheral Lymphedema: 2016 Consensus Document of the International Society of Lymphology. Lymphology. 2016;49:170–184. [PubMed: 29908550]
9. Kim W, Chung SG, Kim TW, et al. Measurement of soft tissue compliance with pressure using ultrasonography. Lymphology. 2008;41:167–177. [PubMed: 19306663]
10. Tomczak H, Nyka W, Lass P. Lymphoedema: lymphoscintigraphy versus other diagnostic techniques--a clinician's point of view. Nucl Med Rev Cent East Eur 2005;8:37–43. [PubMed: 15977145]
11. Yoo JS, Chung SH, Lim MC. Computed tomography-based quantitative assessment of lower extremity lymphedema following treatment for gynecologic cancer. J Gynecol Oncol 2017;28:e18. [PubMed: 28028991]

12. Borri M, Gordon KD, Hughes JC, et al. Magnetic Resonance Imaging-Based Assessment of Breast Cancer-Related Lymphoedema Tissue Composition. Invest Radiol 2017;52:554–561. [PubMed: 28538023]
13. Hou G, Li X, Hou B, et al. Lymphangioma on 68Ga-NOTA-Evans Blue PET/MRI. Clin Nucl Med 2018;43:553–555. [PubMed: 29742595]
14. Wang L, Wu X, Wu M, et al. Edema Areas of Calves Measured with Magnetic Resonance Imaging as a Novel Indicator for Early Staging of Lower Extremity Lymphedema. Lymphat Res Biol 2017.
15. Yoshida RY, Kariya S, Ha-Kawa S, et al. Lymphoscintigraphy for Imaging of the Lymphatic Flow Disorders. Tech Vasc Interv Radiol 2016;19:273–276. [PubMed: 27993322]
16. Pfister G, Saesseli B, Hoffmann U, et al. Diameters of lymphatic capillaries in patients with different forms of primary lymphedema. Lymphology. 1990;23:140–144. [PubMed: 2250483]
17. Tsopelas C, Sutton R. Why certain dyes are useful for localizing the sentinel lymph node. J Nucl Med 2002;43:1377–1382. [PubMed: 12368377]
18. Zhang W, Wu P, Li F, et al. Potential Applications of Using 68Ga-Evans Blue PET/CT in the Evaluation of Lymphatic Disorder: Preliminary Observations. Clin Nucl Med 2016;41:302–308. [PubMed: 26859218]
19. Mayrovitz HN. The standard of care for lymphedema: current concepts and physiological considerations. Lymphat Res Biol 2009;7:101–108. [PubMed: 19522678]
20. Ryan M, Stainton MC, Jaconelli C, et al. The experience of lower limb lymphedema for women after treatment for gynecologic cancer. Oncol Nurs Forum 2003;30:417–423. [PubMed: 12719742]
21. Sharkey AR, King SW, Ramsden AJ, et al. Do surgical interventions for limb lymphoedema reduce cellulitis attack frequency? Microsurgery. 2017;37:348–353. [PubMed: 27661464]
22. Hidding JT, Viehoff PB, Beurskens CH, et al. Measurement Properties of Instruments for Measuring of Lymphedema: Systematic Review. Phys Ther 2016;96:1965–1981. [PubMed: 27340195]
23. Campisi CC, Ryan M, Boccardo F, et al. A Single-Site Technique of Multiple Lymphatic-Venous Anastomoses for the Treatment of Peripheral Lymphedema: Long-Term Clinical Outcome. J Reconstr Microsurg 2016;32:42–49. [PubMed: 26029991]
24. Granzow JW, Soderberg JM, Dauphine C. A novel two-stage surgical approach to treat chronic lymphedema. Breast J. 2014;20:420–422. [PubMed: 24943048]
25. Masia J, Pons G, Rodriguez-Bauza E. Barcelona Lymphedema Algorithm for Surgical Treatment in Breast Cancer-Related Lymphedema. J Reconstr Microsurg 2016;32:329–335. [PubMed: 26975564]
26. Chowdhry M, Rozen WM, Griffiths M. Lymphatic mapping and preoperative imaging in the management of post-mastectomy lymphoedema. Gland Surg 2016;5:187–196. [PubMed: 27047786]
27. Crescenzi R, Donahue PMC. Lymphedema evaluation using noninvasive 3T MR lymphangiography. 2017;46:1349–1360.
28. Zhang J, Lang L, Zhu Z, et al. Clinical Translation of an Albumin-Binding PET Radiotracer 68Ga-NEB. J Nucl Med 2015;56:1609–1614. [PubMed: 26251416]
29. Lohrmann C, Felmerer G, Foeldi E, et al. MR lymphangiography for the assessment of the lymphatic system in patients undergoing microsurgical reconstructions of lymphatic vessels. Microvasc Res 2008;76:42–45. [PubMed: 18456290]
30. Hoffner M, Peterson P, Mansson S, et al. Lymphedema Leads to Fat Deposition in Muscle and Decreased Muscle/Water Volume After Liposuction: A Magnetic Resonance Imaging Study. Lymphat Res Biol 2017.
31. Szuba A, Shin WS, Strauss HW, et al. The third circulation: radionuclide lymphoscintigraphy in the evaluation of lymphedema. J Nucl Med 2003;44:43–57. [PubMed: 12515876]
32. Weissleder H, Weissleder R. Lymphedema: evaluation of qualitative and quantitative lymphoscintigraphy in 238 patients. Radiology. 1988;167:729–735. [PubMed: 3363131]
33. Stanton AW, Modi S, Mellor RH, et al. A quantitative lymphoscintigraphic evaluation of lymphatic function in the swollen hands of women with lymphoedema following breast cancer treatment. Clin Sci (Lond). 2006;110:553–561. [PubMed: 16343054]

34. Yoo JN, Cheong YS, Min YS, et al. Validity of Quantitative Lymphoscintigraphy as a Lymphedema Assessment Tool for Patients With Breast Cancer. Ann Rehabil Med 2015;39:931–940. [PubMed: 26798607]

35. Maclellan RA, Zurakowski D, Voss S, et al. Correlation Between Lymphedema Disease Severity and Lymphoscintigraphic Findings: A Clinical-Radiologic Study. J Am Coll Surg 2017;225:366–370. [PubMed: 28669886]

36. Astrom KG, Abdsaleh S, Brenning GC, et al. MR imaging of primary, secondary, and mixed forms of lymphedema. Acta Radiol 2001;42:409–416. [PubMed: 11442467]

37. Tiwari A, Cheng KS, Button M, et al. Differential diagnosis, investigation, and current treatment of lower limb lymphedema. Arch Surg 2003;138:152–161. [PubMed: 12578410]

38. Tiwari P, Coriddi M, Salani R, et al. Breast and gynecologic cancer-related extremity lymphedema: a review of diagnostic modalities and management options. World J Surg Oncol 2013;11:237. [PubMed: 24053624]

39. Narushima M, Yamamoto T, Ogata F, et al. Indocyanine Green Lymphography Findings in Limb Lymphedema. J Reconstr Microsurg 2016;32:72–79. [PubMed: 26422172]

40. Hayes S, Cornish B, Newman B. Comparison of methods to diagnose lymphoedema among breast cancer survivors: 6-month follow-up. Breast Cancer Res Treat 2005;89:221–226. [PubMed: 15754119]

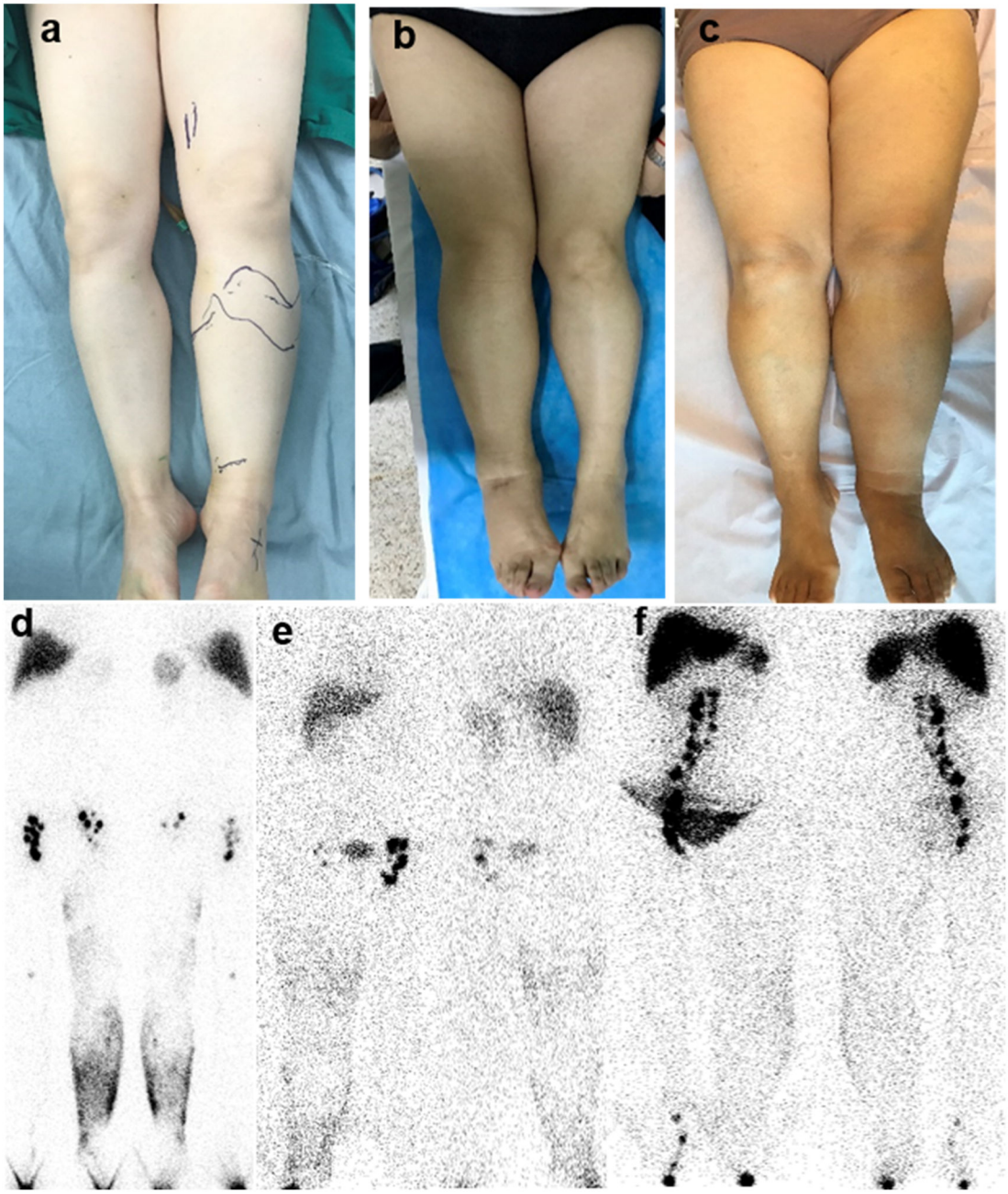


**Fig. 1.**

(a) A 50-year-old female patient had lymphedema in the left lower limb for 2 years (minimal group). (b) A 54-year-old female patient had lymphedema in the right lower extremity for 4 years (moderate group). (c) A 57-year-old female patient had lymphedema in the left lower limb for 2 years (severe group). (a-c) Observed by vision, the swelling level gradually increased from the minimal group to the severe group. (d) $^{99m}$Tc-SC lymphoscintigraphy was performed 6 hours after subcutaneous injection of the radiotracer, showing dermal backflow in the left extremity and reduced visualization of the left inguinal lymph nodes. (e) $^{99m}$Tc-SC lymphoscintigraphy was performed 6 hours after subcutaneous injection of

$^{99m}$Tc-SC, revealing dermal backflow in the right limb and decreased tracer uptake in the right inguinal lymph nodes. (f) $^{99m}$Tc-SC lymphoscintigraphy indicated dermal backflow in the left limb and decreased tracer uptake in the left inguinal lymph nodes.

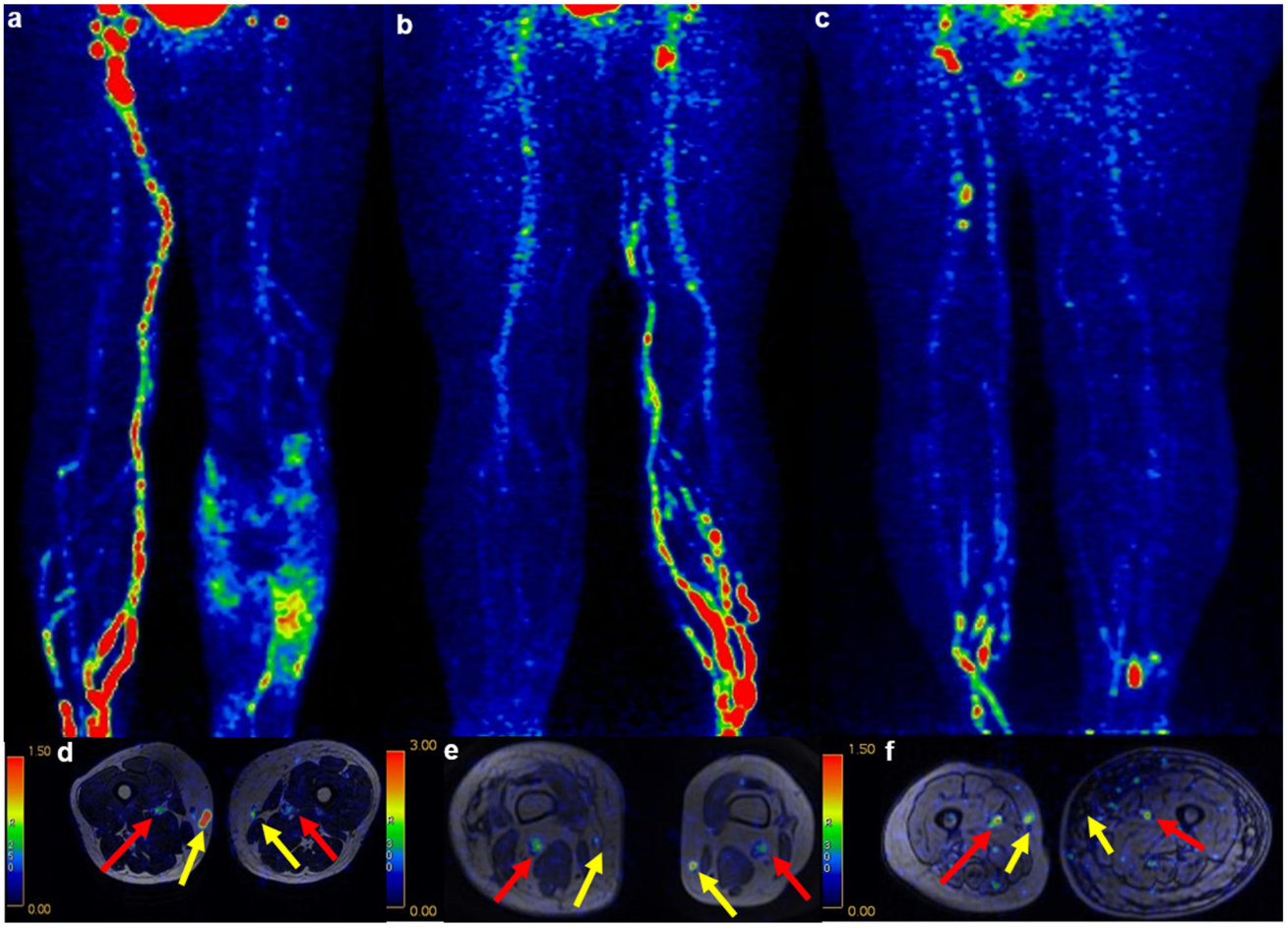


**Fig. 2.**

(a-f) $^{68}$Ga-NEB TOF PET/MR lymphoscintigraphy presented the visualization of DLVs (red arrow) and SLVs (yellow arrow). The lymphatic circulation of the lower extremity could be observed on MIP (a and d, minimal group; b and e, moderate group; c and f, severe group). (a) The PET image showed dermal flowback and reduced inguinal lymph node visualization 20 mins after injection. (b) The PET image 20 mins after subcutaneous injection revealed dermal flowback and decreased inguinal lymph node visualization. (c) The PET image 20 mins after subcutaneous injection showed dermal flowback and decreased inguinal lymph node visualization. (d-f) The axial fusion images indicated that the $^{68}$Ga-NEB accumulation in the SLVs of the affected limb was less than that of the normal limb (yellow arrows), and the $^{68}$Ga-NEB accumulation in the DLVs of the affected limb was equal to that of the normal limb (red arrows). There was also much more adipose fat deposition around the SLV than around the DLV.

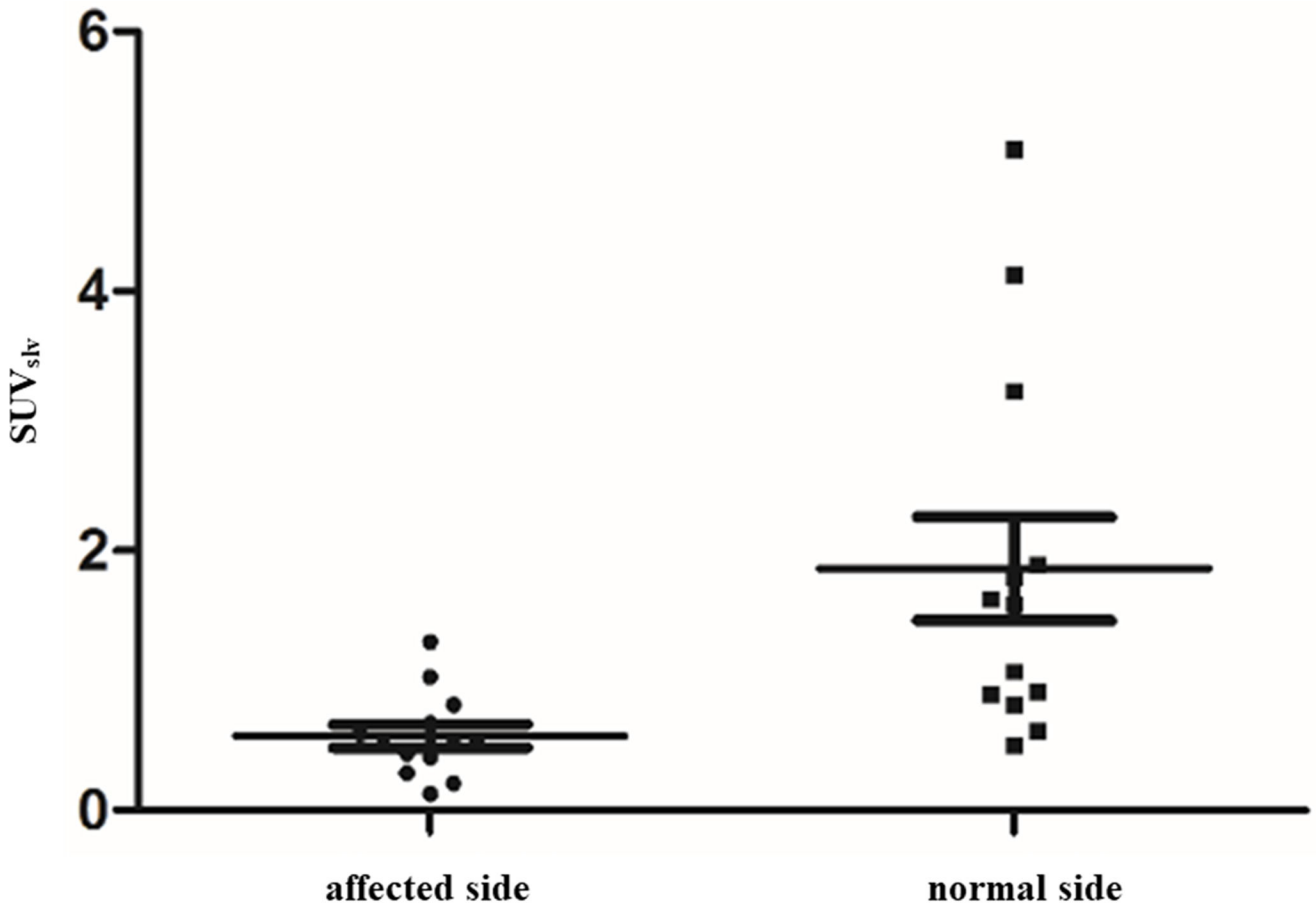


**Fig. 3.**

There was a significant difference between the $SUV_{slv}$ of the affected limb and normal limb ($P<0.05$).

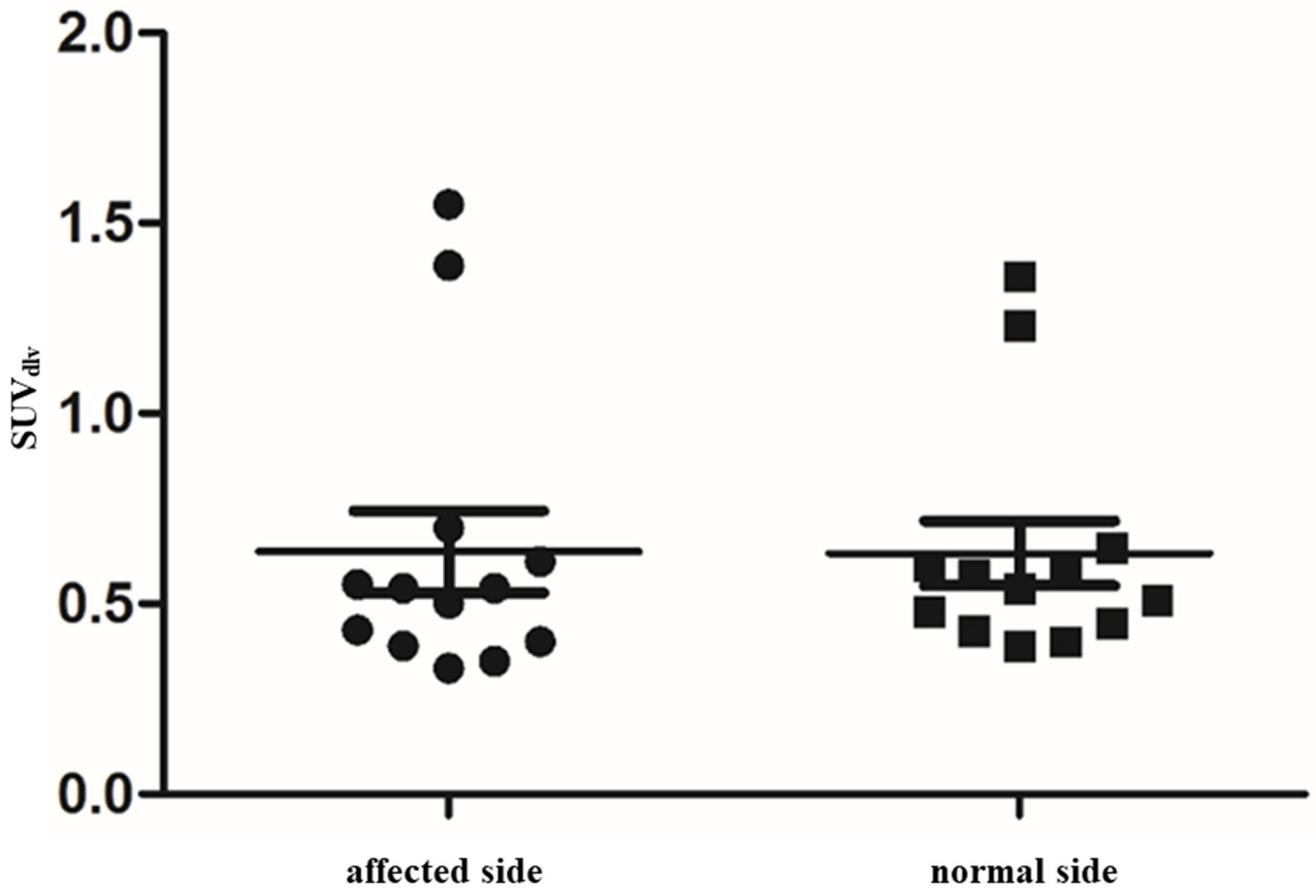


**Fig. 4.**

No significant difference was found between the $SUV_{dlv}$ of the affected limb and normal limb ($P>0.1$).

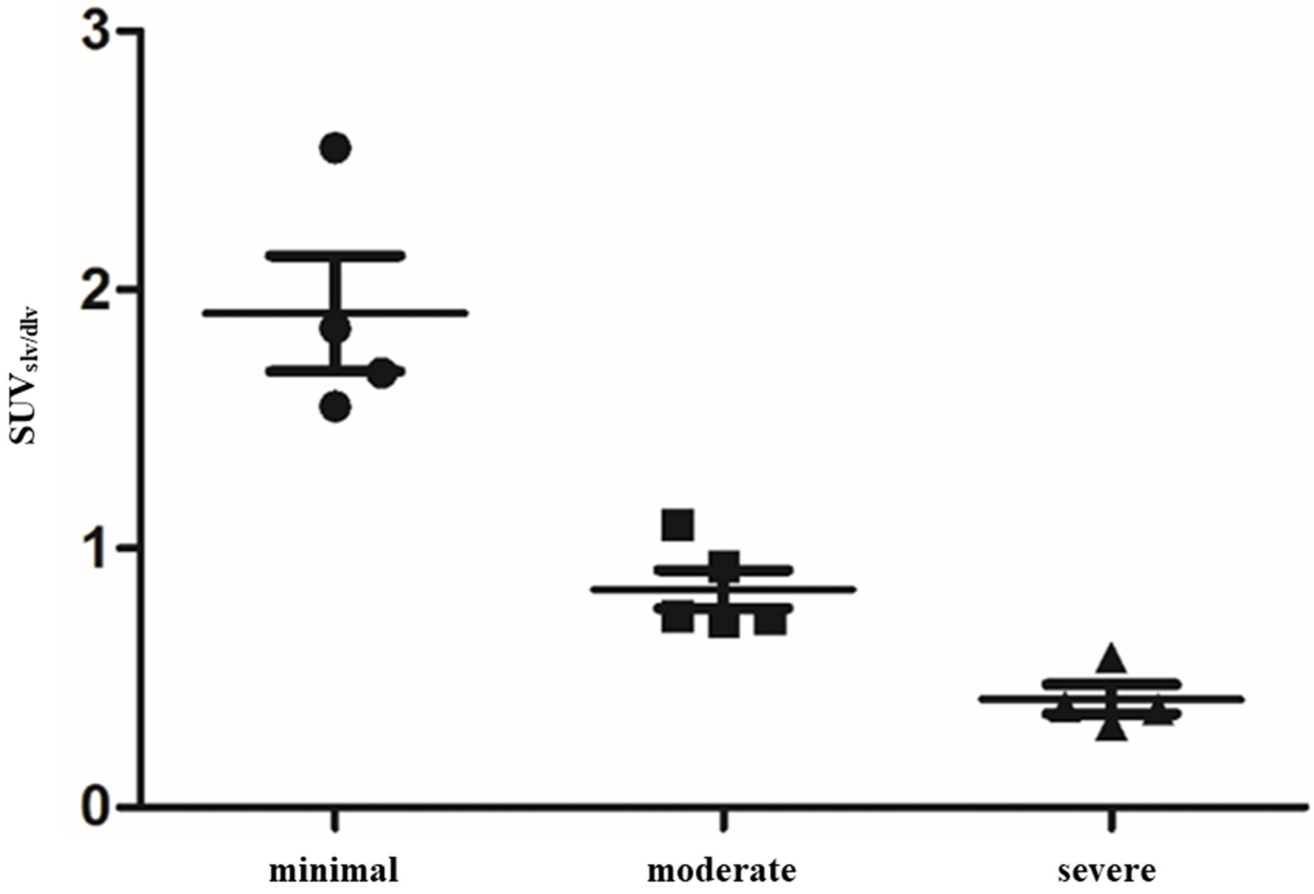


**Fig. 5.**

The $SUV_{slv/dlv}$ of the affected limb showed statistical differences among all three groups ($P<0.05$). The statistical analysis revealed a negative correlation between the $SUV_{slv/dlv}$ and severity of lymphedema ($r = -0.899$, $P<0.01$).

**Table 1**

The information of patients and SUVs of lymphatic

| Lymphedema Severity | Patients | Age | sex | Cause | Time (year) | Affected $SUV_{slv}$ | Normal $SUV_{slv}$ | Affected $SUV_{dlv}$ | Normal $SUV_{dlv}$ | $SUV_{slv/dlv}$ | administered dosage (MBq) | time from injection to imaging(min) | duration of imaging(min) |
|---|---|---|---|---|---|---|---|---|---|---|---|---|---|
| Minimal group | 1 | 54 | F | Intrapelvic surgery | 1 | 0.67±0.43(0.39-1.16) | 1.80±0.45(1.53-2.32) | 0.43±0.08(0.36-0.52) | 0.40±0.01(0.39-0.41) | 1.55 | 37MBq/foot | 20 | 20 |
| | 2 | 42 | F | Ditto | 2 | 1.03±0.76(0.54-1.90) | 3.23±2.87(0.93-6.45) | 0.40±0.03(0.37-0.43) | 0.39±0.09(0.30-0.47) | 2.55 | Ditto | 20 | 20 |
| | 3 | 53 | F | Ditto | 1.5 | 0.59±0.25(0.34-0.84) | 1.07±0.44(0.72-1.57) | 0.35±0.07(0.29-0.43) | 0.51±0.17(0.32-0.66) | 1.68 | Ditto | 20 | 20 |
| | 4 | 50 | F | Ditto | 2 | 1.30±1.17(0.54-2.65) | 5.09±4.80(1.76-10.59) | 0.70±0.33(0.34-0.97) | 0.58±0.10(0.49-0.69) | 1.85 | Ditto | 20 | 20 |
| | *x±s* | 49.75±5.44 | | | 1.63±0.48 | | | | | 1.91±0.45 | | | |
| Moderate group | 5 | 27 | F | unknown | 0.5 | 0.44±0.07(0.40-0.52) | 1.90±0.70(1.38-2.69) | 0.61±0.22(0.48-0.86) | 0.60±0.15(0.45-0.75) | 0.72 | 37MBq/foot | 20 | 20 |
| | 6 | 39 | F | Intrapelvic surgery | 3.5 | 0.50±0.04(0.46-0.54) | 0.82±0.32(0.57-1.18) | 0.54±0.26(0.28-0.79) | 0.65±0.38(0.40-1.09) | 0.93 | Ditto | 20 | 20 |
| | 7 | 47 | F | Ditto | 0.5 | 0.54±0.20(0.35-0.75) | 0.91±0.18(0.71-1.07) | 0.5±0.05(0.44-0.54) | 0.48±0.12(0.36-0.59) | 1.09 | Ditto | 20 | 20 |
| | 8 | 38 | F | Ditto | 2 | 0.29±0.06(0.25-0.35) | 1.59±0.47(1.06-1.97) | 0.39±0.09(0.29-0.46) | 0.45±0.11(0.36-0.57) | 0.73 | Ditto | 20 | 20 |
| | 9 | 54 | F | Ditto | 6 | 0.41±0.13(0.26-0.50) | 1.63±0.81(0.87-2.48) | 0.55±0.09(0.49-0.65) | 0.60±0.35(0.32-0.99) | 0.74 | Ditto | 20 | 20 |
| | *x±s* | 41.00±10.17 | | | 2.50±2.32 | | | | | 0.84±0.16 | | | |
| Severe group | 10 | 54 | F | Intrapelvic surgery | 4 | 0.50±0.10(0.40-0.60) | 4.13±0.28(3.86-4.42) | 1.55±0.47(1.06-1.99) | 1.36±0.22(1.12-1.56) | 0.32 | 37MBq/foot | 20 | 20 |
| | 11 | 57 | F | Ditto | 2 | 0.21±0.12(0.11-0.34) | 0.61±0.08(0.56-0.70) | 0.54±0.14(0.44-0.70) | 0.54±0.13(0.40-0.65) | 0.39 | Ditto | 20 | 20 |
| | 12 | 59 | F | Ditto | 3 | 0.81±0.32(0.48-1.11) | 0.90±0.36(0.50-1.19) | 1.39±0.34(1.03-1.69) | 1.23±0.01(1.22-1.24) | 0.58 | Ditto | 20 | 20 |
| | 13 | 58 | F | Ditto | 3 | 0.13±0.04(0.09-0.17) | 0.50±0.23(0.25-0.71) | 0.33±0.12(0.23-0.46) | 0.43±0.08(0.38-0.53) | 0.38 | Ditto | 20 | 20 |
| | *x±s* | 57.00±2.20 | | | 3.00±0.80 | | | | | 0.42±0.11 | | | |

**Table 2**

Lymph nodes scintigraphy and dermal backflow of affected extremities on $^{68}$Ga-NEB TOF PET/MR

| | minimal | moderate | severe |
|---|---|---|---|
| No. of affected extremities, n (%) | 4 | 5 | 4 |
| Reduced tracer accumulation of lymph nodes, n (%) | 4(100) | 5(100) | 4(100) |
| dermal backflow, n (%) | 3(75) | 3(60) | 2(50) |